AN INDICATION FOR DECONFINEMENT IN Au+Au COLLISIONS AT RHIC*

M. Csanád[1], T. Csörgő[2], B. Lörstad[3] and A. Ster[2]

[1] Dept. Atomic Physics, ELTE, H-1117 Budapest, Pázmány P. 1/a, Hungary
[2] MTA KFKI RMKI, H - 1525 Budapest 114, POBox 49, Hungary
[3] Dept. Physics, University of Lund, S - 22362 Lund, Sweden

We present simultaneous, quality fits to final BRAHMS, PHENIX, PHOBOS and STAR data on particle spectra and two-particle Bose-Einstein or HBT correlations as measured in Au+Au collisions at $\sqrt{s_{NN}} = 130$ GeV. Using the Buda-Lund hydro model, the best fit is achieved when the most central 1/8th of the particle emitting volume is superheated to $T > T_c = 170$ MeV. In contrast, we find no indication for such a hot central region in a similar analysis of Pb+Pb data at CERN SPS.

PACS numbers: 24.10.Nz, 25.75.-q, 25.75.Nq, 25.75.Gz

1. Introduction

Recently, Fodor and Katz calculated the phase diagram of lattice QCD at finite net barion density [1]. The results, obtained with light quark masses about four times heavier than the physical value, indicated that in the $0 \leq \mu_B \leq 200$ MeV region the transition from confined to deconfined matter is a cross-over, with $T_c \simeq 172 \pm 3$ MeV which is, within errors, independent of the bariochemical potential in this region. At the same time, deconfined matter is searched for in Pb+Pb collisions with laboratory bombarding energies of 158 AGeV at CERN SPS as well as in Au + Au collisions at RHIC, with $\sqrt{s_{NN}} = 200$ GeV colliding energies.

2. Basic properties of the Buda-Lund hydro model

Here we report on an analysis of the measured single particle spectra and two-particle Bose-Einstein correlation functions using the Buda-Lund hydrodynamical model [2, 3]. The key features of this model can be summarized as follows.

* Presented at XXXIIIth Int. Symp. Multipart. Dyn. Cracow, Poland, 9/5-11/2003

1) The particle emitting source is assumed to have a core-halo structure [5], where the particle production in the core is governed by local thermalization and relativistic, three-dimensional expansion, while particle production in the halo is governed by the decays of long-lived hadronic resonances, that have lifetimes larger, or much larger than the characteristic 5-10 fm/c lifetimes of the hydrodynamically evolving core. In case of pion production, such resonances are e.g. ω, η and η'.

2) The freeze-out distribution of the core is described by a three - dimensionally expanding, locally thermalized source, that reflects the symmetry properties of the collision (axial symmetry for central collisions).

3) The model goes back to known solutions of (relativistic) hydrodynamics in limiting cases when such solutions are known (e.g. non-relativistic or ultrarelativistic limits).

4) The flow field has a transverse and a longitudinal Hubble flow, the density and the inverse temperature distributions are parameterized keeping the means and variances of these distributions only, in such a form that all the observables can be calculated analytically from the model.

5) If the flow vanishes and the temperature and density are constants, the freeze-out temperature can be determined from the single-particle spectra and the geometrical sizes of the source from two-particle Bose-Einstein correlations. However, in the limit of a large, strongly expanding source with local temperature inhomogeneities, the two-particle correlations are dominated by thermal length scales (sizes within which the Boltzmann factor is nearly constant), and the single particle spectra contain (or even are dominated) by flow and temperature inhomogeneity effects, corresponding to a scaling limiting behaviour.

6) In the scaling limit, the analytic formulas given in refs. [2, 3, 4] yield the analytic prediction that $R_{out} \simeq R_{side} \simeq R_{long} \propto 1/\sqrt{m_t}$, or, with other words, $R_{out}/R_{side} \simeq R_{side}/R_{long} \simeq R_{long}/R_{out} \simeq 1$, where the equality is reached for sufficiently large transverse masses, satisfying $m_t \gg T_0$, and at lower m_t the model predicts scaling violating correction terms.

This Buda-Lund hydro model and the above mentioned analytic formulas were recently reviewed and summarized in ref. [4], as far as the single particle spectra and the two-particle Bose-Einstein or HBT radius parameters are concerned. Since at RHIC the BRAHMS and the PHOBOS collaborations reported data on the pseudo-rapidity distributions in refs. [7, 8], we have extended this model and have improved the analytic calculation in such a way, that in the longitudinal, space-time rapidity variable, the position of the point of maximal emittivity can be found exactly now, and thus analytic calculation is not anymore limited by the linearized saddle-point equations.

3. Fits to final run-1 Au+Au data at RHIC

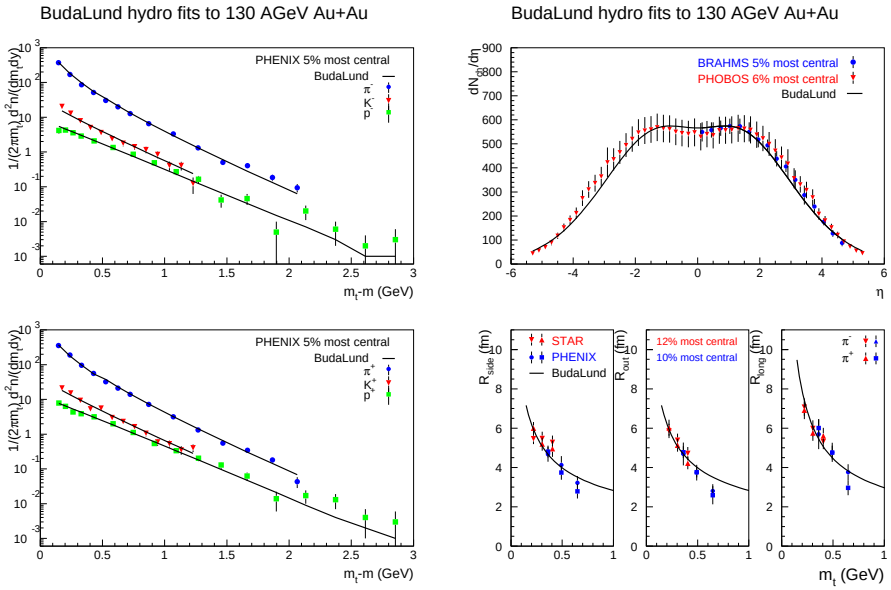

Fig. 1. Solid line shows the simultaneous Buda-Lund fit to final Au+Au data at $\sqrt{s_{NN}} = 130$ GeV, vers. 1.5. The transverse mass distributions are measured by PHENIX [9], the pseudorapidity distributions of charged particles are measured by BRAHMS [7] and PHOBOS [8], while the transverse mass dependence of the radius parameters are measured by STAR [11] and PHENIX [10].

BL parameter	Au+Au RHIC	Pb+Pb ⟨SPS⟩	h+p SPS
T_0 [MeV]	214 ± 7	139 ± 6	140 ± 3
$\langle u_t \rangle$	1.0 ± 0.1	0.55 ± 0.06	0.20 ± 0.07
$R_{s\|G}$ [fm]	8.6 ± 0.4	7.1 ± 0.2	7.3 ± 0.8
τ_0 [fm/c]	6.0 ± 0.2	5.9 ± 0.6	1.4 ± 0.1
$\Delta\tau$ [fm/c]	0.3 ± 1.2	1.6 ± 1.5	1.36 ± 0.02
$\Delta\eta$	2.3 ± 0.4	2.1 ± 0.4	1.36 ± 0.02
T_S [MeV]	0.5 T_0 fixed	131 ± 8	82 ± 7
T_e [MeV]	102 ± 11	87 ± 24	0.1 ± 0.1

Table 1. Source parameters from simultaneous fits of final BRAHMS, PHENIX, PHOBOS and STAR data for $Au + Au$ collisions at $\sqrt{s_{NN}} = 130$ GeV data, as given in Fig. 1, obtained with the Buda-Lund hydrodynamical model, version 1.5. Pb+Pb data were fitted in ref. [13], while h+p data at CERN SPS in ref. [14].

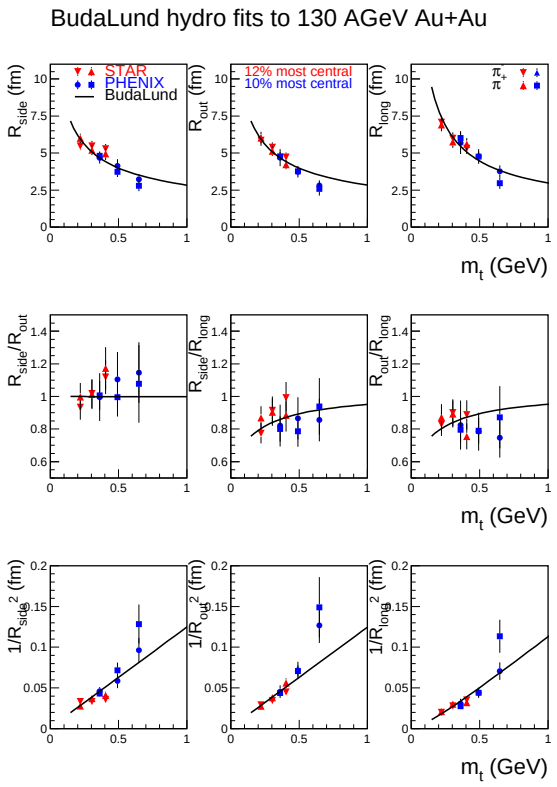

Fig. 2. Top row shows the transverse mass dependence of the side, out and longitudinal HBT radii, the central line shows their pairwise ratio (usually only $R_{\rm out}/R_{\rm side}$ is shown) together with the Buda-Lund fits, vers. 1.5. The bottom line shows the inverse of the squared radii. The intercept of the curves in this row is within errors zero for the two transverse components, so the fugacity is independent of the transverse coordinates. As the intercept is nonzero in the longitudinal direction, the fugacity (hence particle ratios) are rapidity dependent.

In this analysis, final BRAHMS [7], PHENIX [9, 10], PHOBOS [8], and STAR [11] data are used, and all these datapoints were fitted simultaneously, using the analytic expressions and the CERN Minuit fitting package. The fitting package used in this analysis is version 1.5, made public at [6]. A well defined minimum was found, with accurate error matrix and a statistically acceptable fit quality. The results are shown on Fig. 1 and the essential parameters are summarized in Table 1. In addition to the parameters in Table 1, we have 6 chemical potentials that regulate the absolute normalization

of the single particle spectra of $\pi^{\pm}$, $K^{\pm}$, and $p^{\pm}$. The quality of the fit to the RHIC data is characterized by $\chi^2/\mathrm{NDF}= 158/180$, that corresponds to a confidence level of 88 %. More details are given in ref. [12]. Here we note only, that the net baryochemical potential, μ_B can be determined from the difference of the proton and antiproton chemical potentials. In our case, this value is $\mu_B = 77 \pm 38$ MeV, well within the range where the critical temperature is within errors independent of the baryochemical potential according to ref. [1]. The fitting of RHIC data turned out to be more complicated than that to the CERN SPS NA44, NA49 and WA98 data, given in ref. [13]. The reason was that the RHIC HBT correlation data are closer to the scaling limiting case than the data at CERN SPS. This implied that the fugacity distribution, $\exp(\mu(x)/T(x))$ becomes a constant parameter at RHIC, within resolvable errors, independently of the transverse coordinate values. Hence the "geometric" contribution to the HBT radius parameters is negligibly small. The finite transverse size seems to be generated by the finite transverse size of the hot region, but the fugacity term is within the resolvable errors independent of the transverse coordinates in this region. This is signalled by the fact that the fits became independent of the geometrical source sizes, R_G, which characterizes the transverse variations of the fugacity term, and we observed that R_G becomes an irrelevant parameter at RHIC, with $1/R_G^2 \approx 0$. This can be seen in the lower plots of Fig. 2, where we show the inverse squared radii versus m_t. The Buda-Lund model predicted, see eqs. (53-58) in ref. [2] and also eqs. (26-28) in [15], that the linearity of the inverse radii as a function of m_t can be connected to the Hubble flow and the temperature gradients. The slopes are the same for side, out and longitudinal radii if the Hubble flow (and the temperature inhomogeneities) become direction independent. The intercepts of the linearly extrapolated m_t dependent inverse squared radii at $m_t = 0$ determine $1/R_G^2$, or the magnitude of corrections from the finite geometrical source sizes, that stem from the $\exp(\mu(x)/T(x))$ terms. We can see on Fig. 3, that these corrections within errors vanish at RHIC. This result is important, because it explains, why thermal and statistical models can be successful at RHIC: if $\exp(\mu(x)/T(x)) = \exp(\mu_0/T_0)$, then this factor becomes an overall normalization factor, proportional to the particle abundances. Indeed, we found that when the finite size in the transverse direction is generated by the $T(x)$ distribution, the quality of the fit increased and we had no degenerate parameters in the fit any more. In Table 1, we determined R_s at RHIC by the condition, that $T(r_x = r_y = R_s) = T_0/2$.

On the other hand we have obtained similarly good description of these data if we require that the four-velocity field is a fully developed, three-dimensional Hubble flow, with $u^\mu = x^\mu/\tau$, however, we cannot elaborate on this point here due to the space limitations [16].

4. Conclusions

Table 1 and Figures 1 and 2 indicate that there is no real HBT puzzle at RHIC- the Buda-Lund hydro model works here as well as at CERN SPS, and gives a good quality description of the transverse mass dependence of the HBT radii. For the dynamical reason, see refs. [15] and [2]. Naturally, we find that the transverse size of the source is larger and the transverse flow is stronger in heavy ion collisions than in h+p collisions. We also observe, that the central temperature, $T_0 = 214 \pm 7$ MeV, is significantly higher at RHIC, than the critical temperature, $T_c = 172 \pm 3$ MeV, calculated from lattice QCD, and this is a significant, more than 5 standard deviation effect. Finding similar parameters from the analysis of the pseudorapidity dependence of the elliptic flow, it was estimated in ref. [16] that about 1/8th of the total volume is above the critical temperature in Au+Au collisions at RHIC at the time when pions are emitted from the source. We interpret this result as an indication for quark deconfinement and a cross-over transition in Au+Au collisions at $\sqrt{s_{NN}} = 130$ GeV at RHIC. A similar conclusion has been first achieved in ref. [17] when analysing the final PHENIX and STAR data on midrapidity spectra and Bose-Einstein correlations, but only at a three standard deviation level. By including the pseudorapidity distributions of BRAHMS and PHOBOS, the significance of the result increased.

REFERENCES

[1] Z. Fodor and S. D. Katz, JHEP **0203** (2002) 014
[2] T. Csörgő and B. Lörstad, Phys. Rev. C **54** (1996) 1390
[3] T. Csörgő and B. Lörstad, Nucl. Phys. A **590** (1995) 465C
[4] T. Csörgő, Heavy Ion Phys. **15** (2002) 1
[5] T. Csörgő, B. Lörstad and J. Zimányi, Z. Phys. C **71** (1996) 491
[6] http://www.kfki.hu/~csorgo/budalund/
[7] I. G. Bearden *et al.* [BRAHMS Collaborations], Phys. Lett. B **523** (2001) 227
[8] B. B. Back *et al.* [PHOBOS Collaboration], Phys. Rev. Lett. **87** (2001) 102303
[9] K. Adcox *et al.* [PHENIX Collaboration], Phys. Rev. Lett. **88** (2002) 242301
[10] K. Adcox *et al.* [PHENIX Collaboration], Phys. Rev. Lett. **88** (2002) 192302
[11] C. Adler *et al.* [STAR Collaboration], Phys. Rev. Lett. **87** (2001) 082301
[12] http://hirg.if.pw.edu.pl/en/meeting/oct2003/talks/csorgo/Ster.ppt
[13] A. Ster, T. Csörgő and B. Lörstad, Nucl. Phys. A **661** (1999) 419
[14] N. M. Agababian *et al.* [EHS/NA22 Coll.], Phys. Lett. B **422** (1998) 359
[15] T. Csörgő and J. Zimányi, Heavy Ion Phys. **17** (2003) 281
[16] M. Csanád, T. Csörgő and B. Lörstad, arXiv:nucl-th/0310040.
[17] T. Csörgő and A. Ster, Heavy Ion Phys. **17** (2003) 295